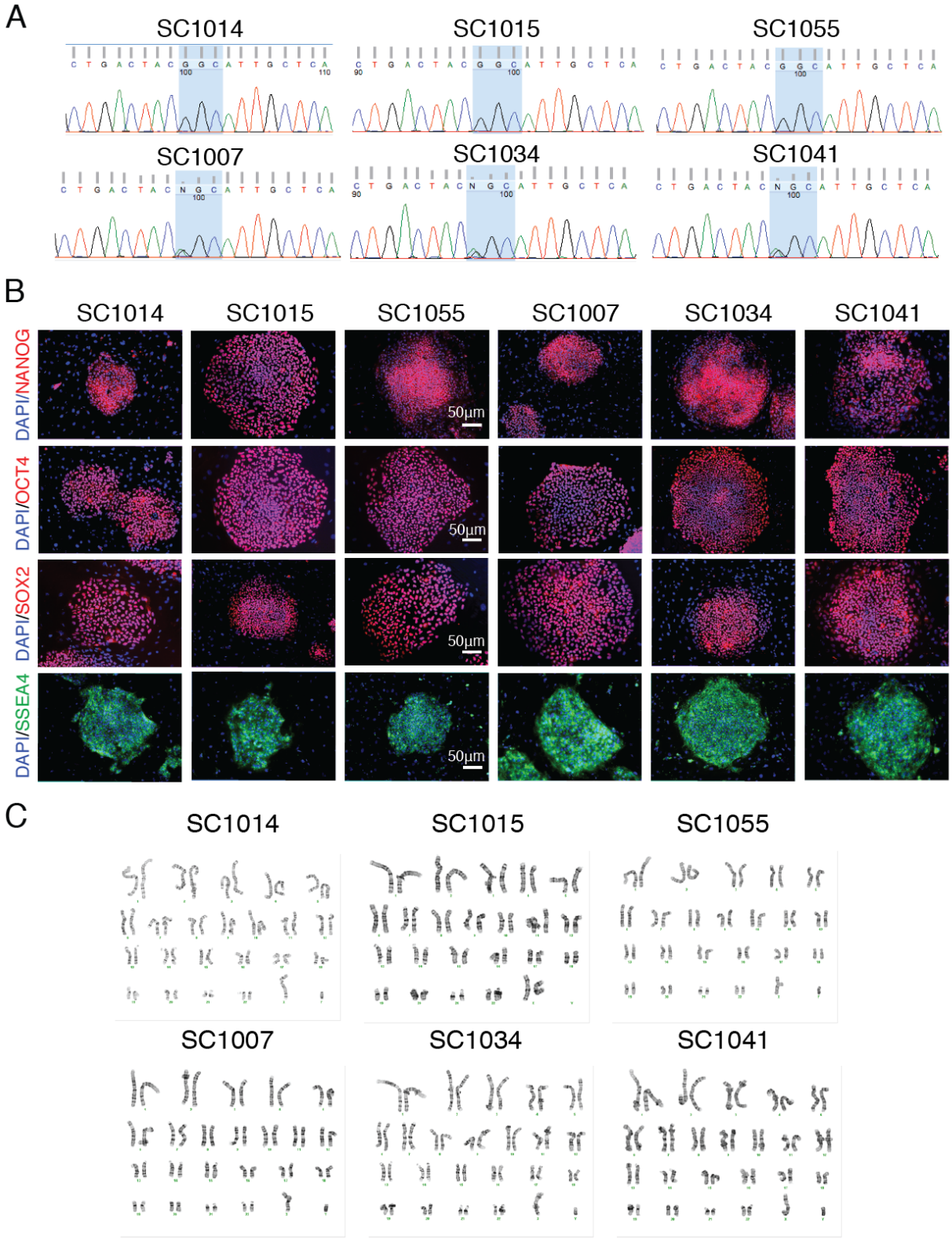

Figure S1. Related to Figure 1. Characterization and differentiation of LRRK2 human iPSC lines
(**A**) G2019S LRRK2 genotyping results of the human iPSC lines used for this study. SC1014, SC1015, SC1055 lines are non-PD control. SC1007, SC1034, SC1041 lines are G2019S LRRK2 heterozygotes (GGC -> AGC). The original fibroblasts were obtained from Mayo Clinic with de-identified patients information. (**B**) Immunocytochemistry shows pluripotent stem cell marker expression in human iPSC lines. All lines show pluripotent stem cell marker (NANOG, OCT4, SOX2, SSEA4) expression. (**C**) Karyotyping of human iPSC lines. All lines have normal karyotypes.

A

Summary of human DA neuron electrophysiological data

Feature	Control	Control + TA S15	GS	GS + TA S15
Rp (MΩ)	4.24 ± 0.56	4.26 ± 0.59	4.27 ± 0.76	4.20 ± 0.62
Rin (MΩ)	194.2 ± 44.0	193.7 ± 35.5	191.0 ± 33.7	187.1 ± 35.2
Rseries (MΩ)	17.14 ± 4.65	18.54 ± 3.74	18.27 ± 5.67	18.96 ± 4.64
Leak (pA)	-11.89 ± 5.42	-10.57 ± 3.84	-11.09 ± 5.52	-10.57 ± 2.20
RMP (mV)	-61.50 ± 2.31	-60.60 ± 3.98	-60.90 ± 3.03	-60.50 ± 3.31

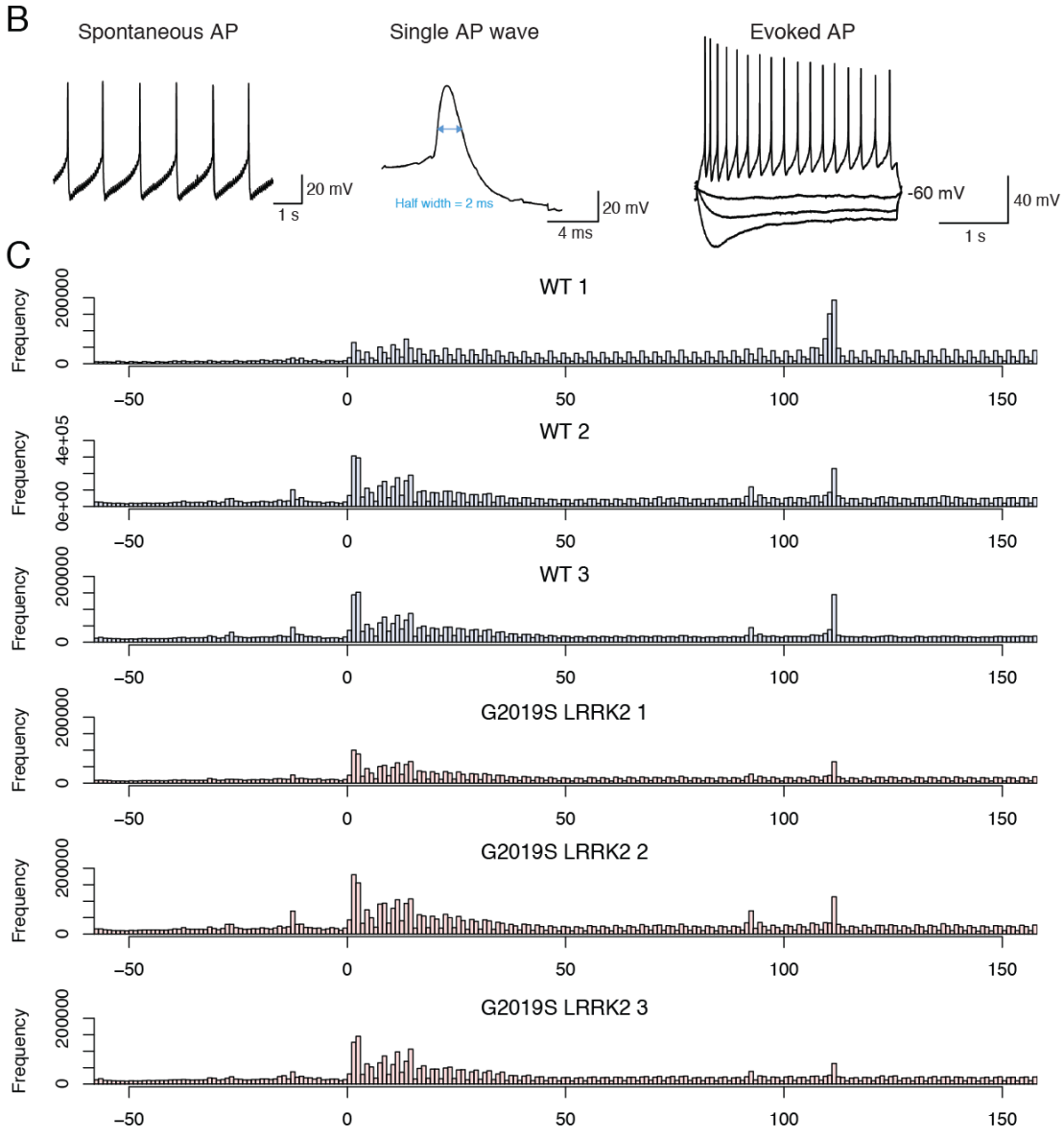

Figure S2. Related to Figures 2 and 3. Electrophysiological characteristics of human DA neurons and ribosome profiling of human DA neurons

(**A**) Electrophysiological characteristics of human iPSCs-derived DA neurons. Rp, pipette resistance; Rin, input resistance; Rseries, series resistance which was typically 10–30 MΩ; Leak, leak current during recording, RMP, resting membrane potential. No significant change in basal characteristics of action potential (AP) generation was found in G2019S LRRK2 DA neurons. (**B**) Representative AP firing pattern in human DA neurons (left), representative AP trace at higher time resolution (middle), representative current-clamp recordings evoked by series of 1000ms current pulses (right). Increased L-VGCC current in GS LRRK2 human DA neurons. (**C**) Triplet periodicity of ribosome footprints from human DA neurons ribosome profiling data. Transcript coordinates of ribosome footprints were calculated based on its 5' end. No significant change in triplet periodicity was observed in GS LRRK2 human DA neurons. WT 1: SC1014; WT 2: SC1015; WT 3: SC1055; GS LRRK2 1: SC1007; GS LRRK2 2: SC1034; GS LRRK2 3: SC1041. WT: wild-type.

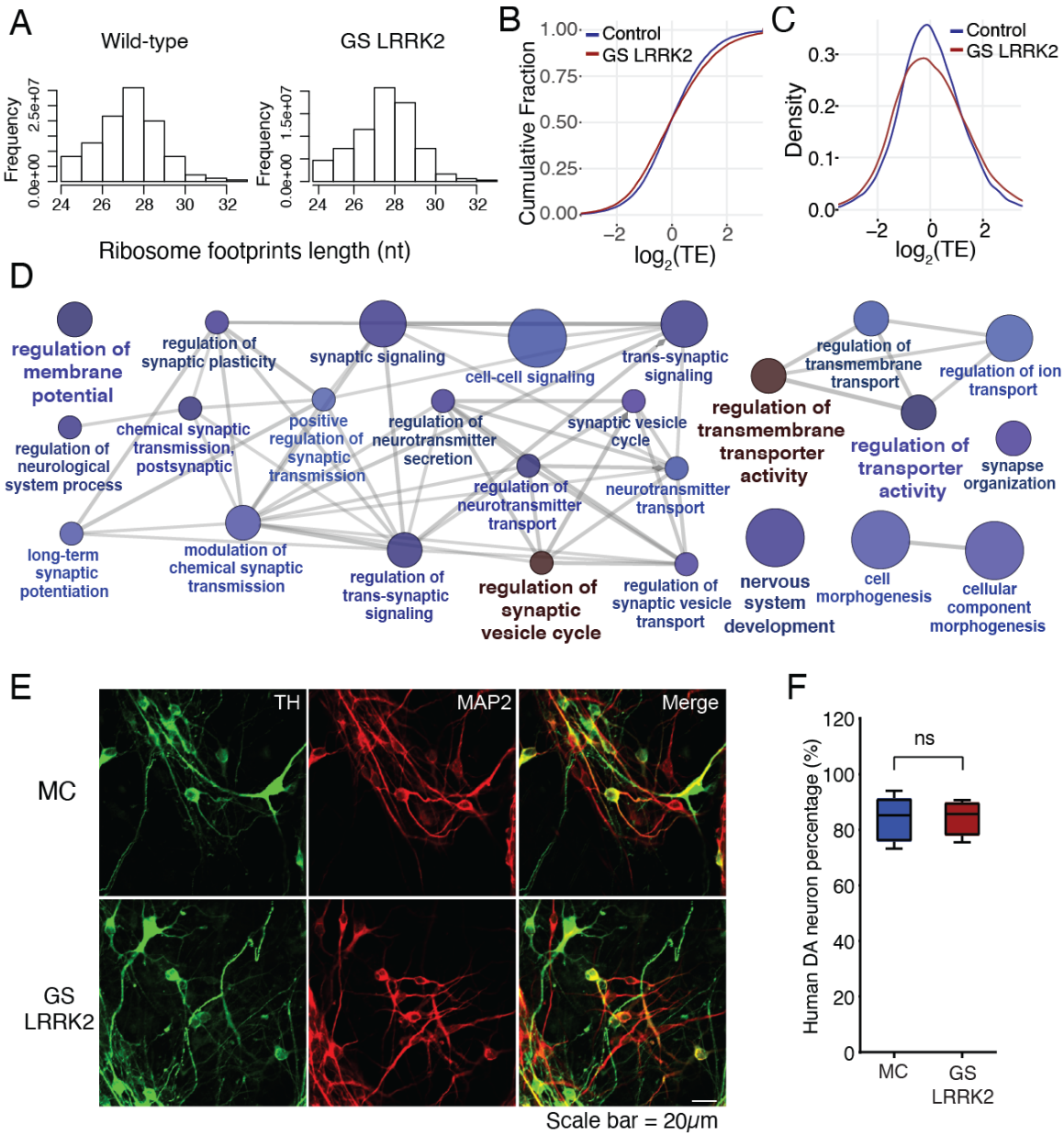

G

Feature	GC	Mutant
Rp (MΩ)	4.08 ± 0.15	4.03 ± 0.13
Rin (MΩ)	236.6 ± 10.76	230.2 ± 8.64
Rseries (MΩ)	17.42 ± 0.97	17.61 ± 0.86
Leak (pA)	-14.14 ± 1.24	-13.94 ± 1.19
RMP (mV)	-60.55 ± 0.77	-59.55 ± 1.05

Figure S3. Related to Figures 1, 2 and 4. Ribosome profiling of human DA neurons and electrophysiological characteristics of an isogenic pair of DA neurons

(**A**) Ribosome footprint length distribution of wild-type control and GS LRRK2 human dopamine neurons. (**B** and **C**) TE distribution profiles in wild-type and GS LRRK2 human DA neurons were compared using cumulative distribution and density plots. These plots demonstrate that GS LRRK2 neurons have a broadly altered TE distribution. All values are in $\log_2$. (**D**) Gene ontology analysis by ClueGO software from the TE up and TE down genes in GS LRRK2 human DA neurons (log2 fold change > 0.8 or < -0.8) (Bindea et al., 2009). Color: GO hierarchy level, size: group size. (**E**) TH and MAP2 staining of mutation-corrected and G2019S LRRK2 isogenic pair human dopamine neurons. (**F**) Quantification of TH positive neurons over MAP2 positive neurons (Student's t-test). (**G**) Electrophysiological characteristics of isogenic DA neurons. Rp, pipette resistance; Rin, input resistance; Rseries, series resistance which was typically 10–30 MΩ; Leak, leak current during recording, RMP, resting membrane potential. GS: G2019S, MC: mutation-corrected.

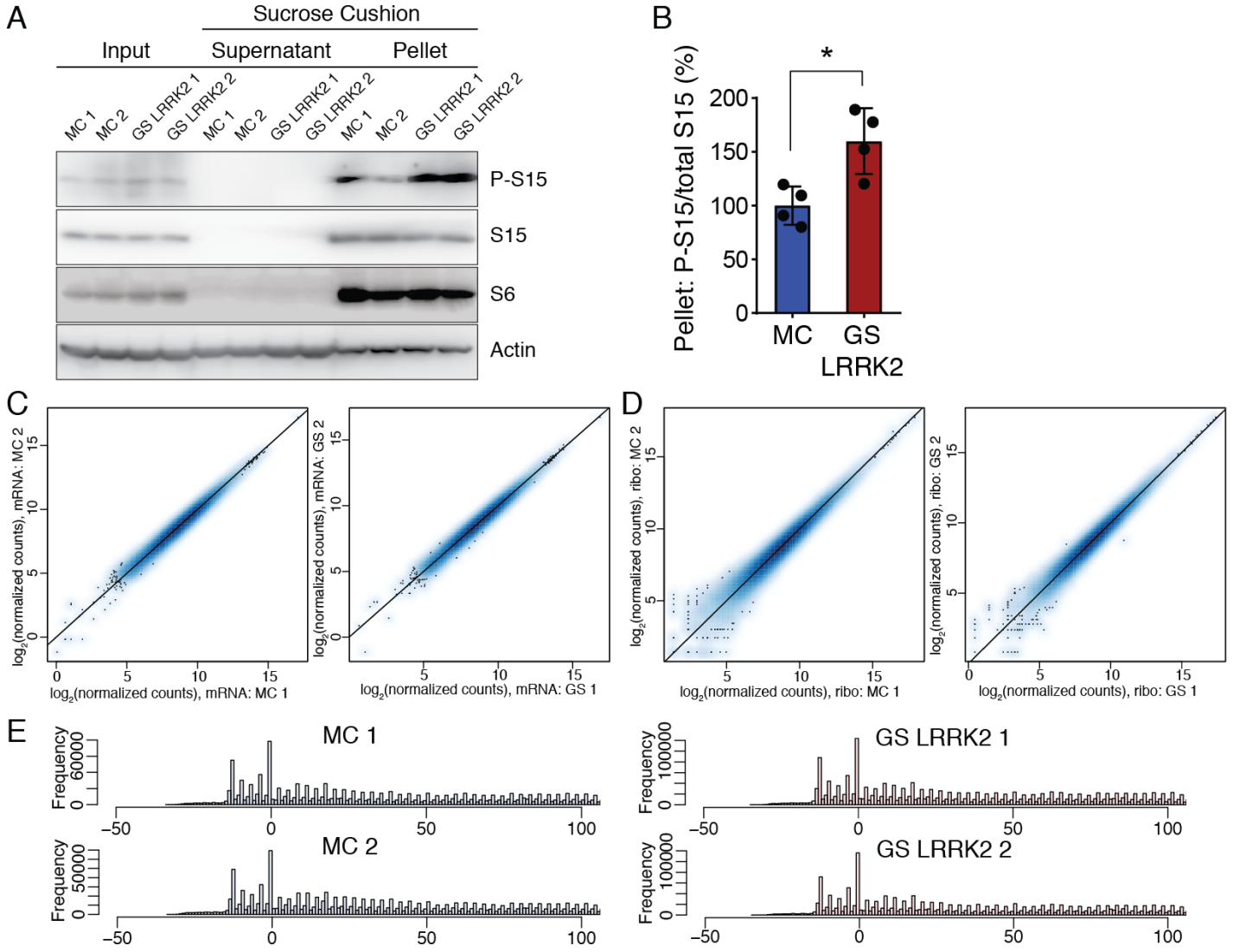

Figure S4. Related to Figure 5. Ribosome profiling of isogenic human DA neurons
(**A** and **B**) Increased phosphorylation of S15 in G2019S LRRK2 human DA neurons. Comparison between mutation-corrected and G2019S LRRK2 DA neurons. n=4 (two independent batches with replicates), Mann-Whitney test (p=0.0286). Sucrose cushion was performed to enrich ribosomal proteins as previously described (Martin et al., 2014b). (**C** and **D**) Normalized counts from replicates were directly compared to check reproducibility between replicates. (C) RNA-seq and (D) ribosome profiling results were compared. Pearson correlation coefficient r= 0.9963 (mRNA, MC), 0.9968 (mRNA, GS LRRK2), 0.9972 (ribo, MC), 0.9987 (ribo, GS LRRK2). Ribo: ribosome profiling. (**E**) Triplet periodicity of ribosome footprints from isogenic DA neurons. Transcript coordinates were calculated based on the footprinting 5' end. No significant change in triplet periodicity was observed in GS LRRK2 human DA neurons. GS: G2019S, MC: mutation-corrected.

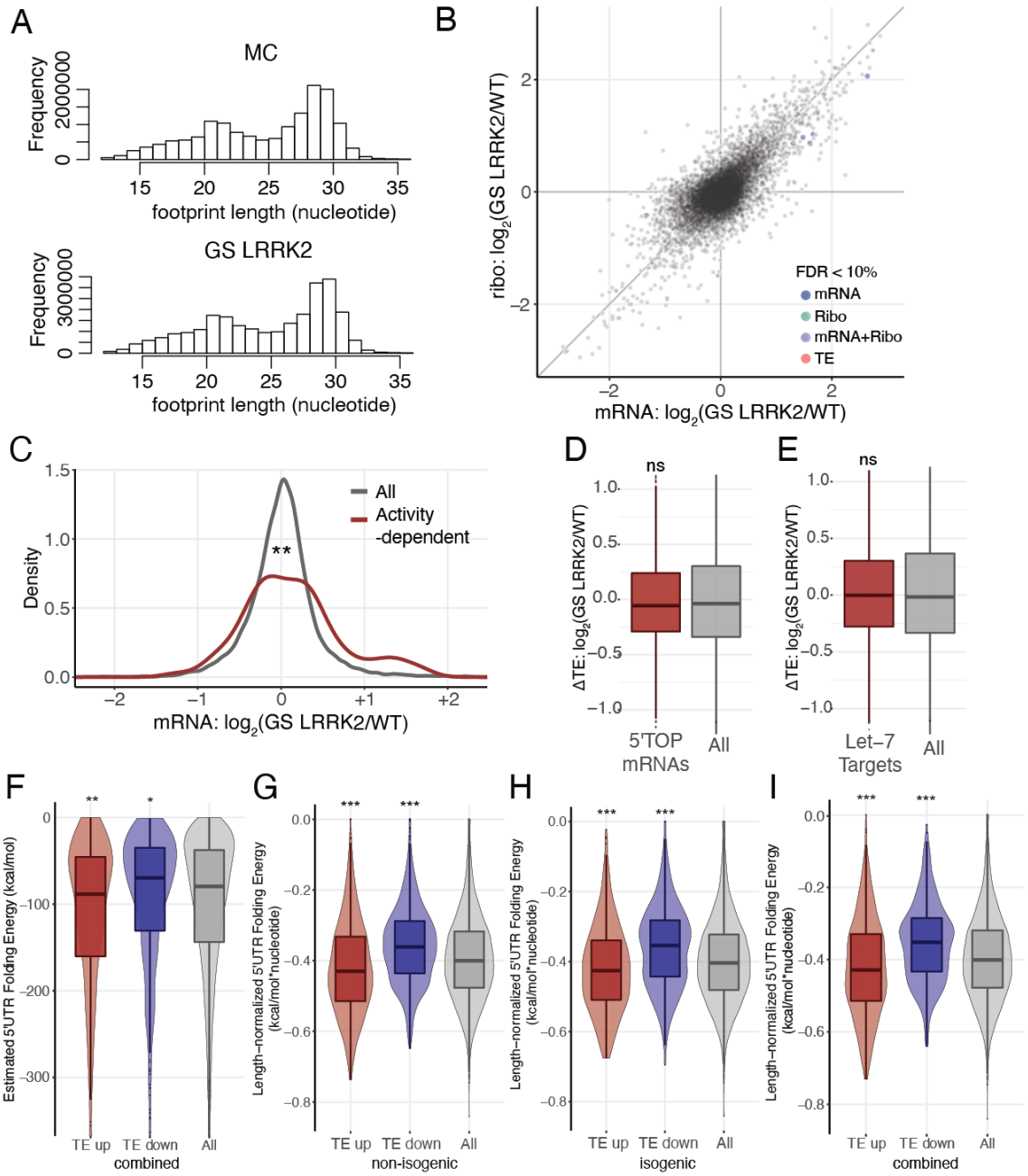

Figure S5. Related to Figures 5 and 6. Correlation between 5'UTR secondary structure and translation efficiency

(**A**) Ribosome footprint length distributions of mutation-corrected and GS LRRK2 human dopamine neurons. (**B**) Scatterplot comparing RNA-seq and ribosome profiling results from combined DESeq2 analysis. Significantly changed genes with FDR < 10% were visualized. All values are in $\log_2$, and each data point represents a single transcript. (**C**) Distribution of activity-dependent genes from combined analysis. Kolmogorov-Smirnov test (p=0.002461). (**D**) TE differences of 5' TOP mRNAs. 5' TOP mRNAs are translationally regulated by mTOR signaling pathway through phosphorylation of 4E-BP (Thoreen et al., 2012). Our data do not support differential regulation of 5' TOP mRNAs in GS LRRK2 human dopamine neurons (Wilcoxon signed-rank test). (**E**) Human let-7 targets were downloaded from the miRWalk 2.0 database. The result indicates that the let-7 target mRNAs are not differentially regulated in GS LRRK2 human dopamine neurons (Wilcoxon signed-rank test). (**F**) Estimated 5'UTR folding energy of TE up and TE down genes (TE > 0.5 or < -0.5, respectively) from combined analysis. Wilcoxon signed-rank test (all comparisons are against all genes control) (p < 0.002692 (TE up), p < 0.01304 (TE down)). (**G** to **I**) TE and 5'UTR correlation with estimated 5'UTR folding energy normalized by the length of 5'UTR. Wilcoxon signed-rank test (all comparisons are against all genes control) ((G): p < 0.0001 (TE up), p < 0.0001 (TE down), (H): p < 0.0001 (TE up), p = 0.0001715 (TE down), (I): p < 0.0001 (TE up), p < 0.0001 (TE down)). GS: G2019S, WT: wild-type, MC: mutation-corrected.

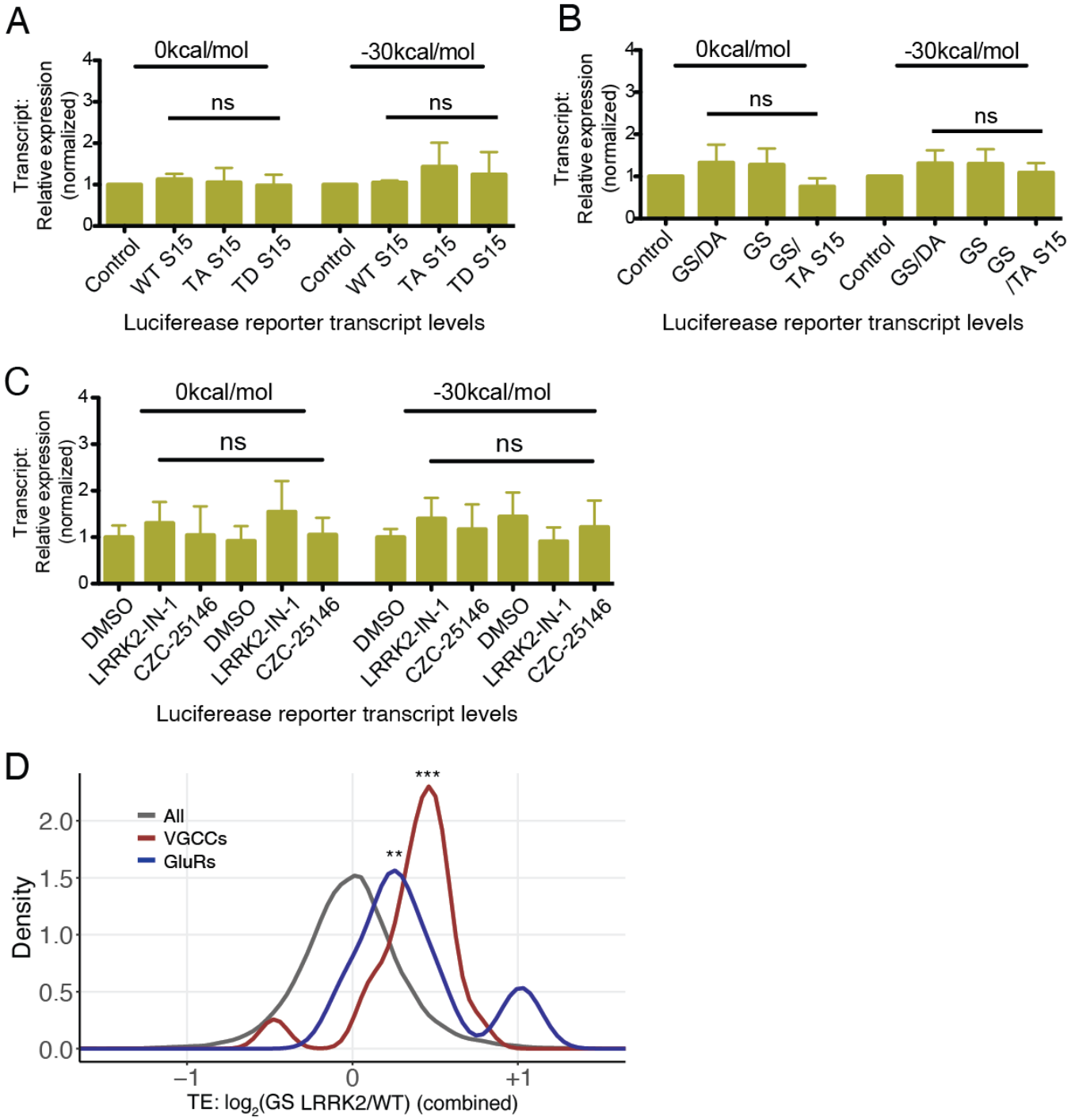

Figure S6. Related to Figures 6 and 7. 5'UTR reporter assays in G2019S LRRK2 expressing neurons
(**A** to **C**) Luciferase transcript levels were measured by qPCR for stem-loop reporter luciferase assays. Control RNA was spiked-in to the lysate and used to normalize the input. Reporter transcript levels were not affected by LRRK2 / S15 expression or LRRK2 inhibitor treatment. One-way ANOVA was used to determine statistical significance. ns = no significance. (**D**) A TE density plot of voltage-gated calcium channel genes (VGCCs, 26 genes) and ionotropic glutamate receptor genes (GluRs, 18 genes) compared to all genes from combined analysis. Wilcoxon signed-rank test (VGCC: $p < 0.001$, GLUR: $p = 0.008318$). GS: G2019S, WT: wild-type, TA: T136A, TD: T136D.

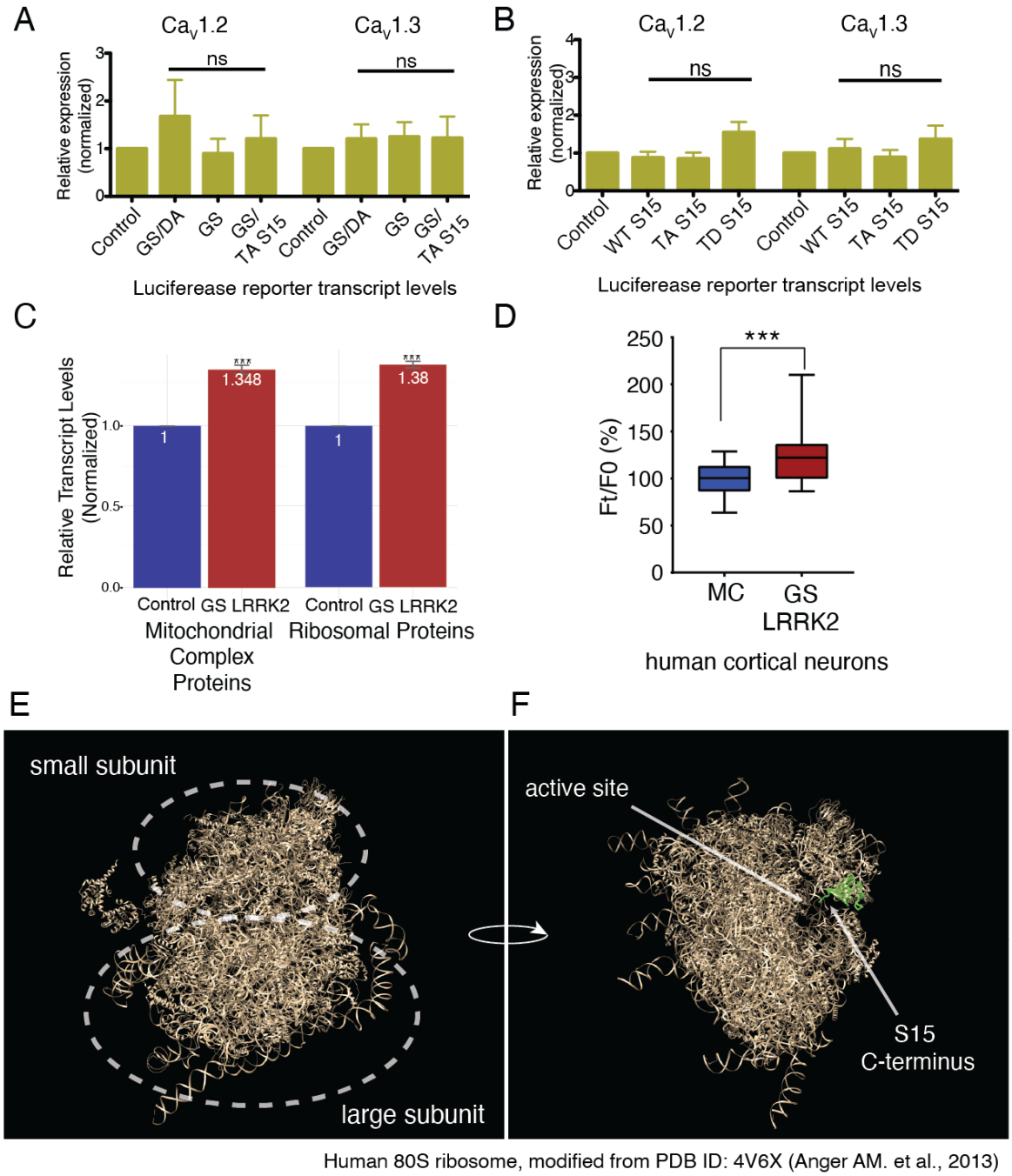

Human 80S ribosome, modified from PDB ID: 4V6X (Anger AM. et al., 2013)

Figure S7. Related to Figure 7. Increased calcium influx and potential effects on metabolism in G2019S LRRK2 expressing neurons

(**A** and **B**) Luciferase transcript levels were measured by qPCR for the L-VGCC 5'UTR reporter (*CACNA1C*, *CACNA1D*) assays. Control RNA was spiked-in to the lysate and used to normalize the input. Transcript levels of the reporter are not affected by LRRK2 or S15 expression. One-way ANOVA was used to determine statistical significance and there was no significant transcript level change detected in all reporter assays. (**C**) Transcript levels of metabolism-related genes (ribosomal proteins, nuclear encoded mitochondrial complex proteins). GS LRRK2 human DA neurons have significantly increased (~35% increase) transcript levels of the two groups (Student's t-test, $p < 0.001$ for both), suggesting that GS LRRK2 DA neurons may have increased metabolic demands. Group sizes: 81 (mitochondrial genes), 85 (ribosomal proteins). (**D**) Intracellular Ca^{2+} levels of an isogenic pair of human cortical neurons were measured by the Fluo-4 Ca^{2+} indicator. 6 - 8 independent measurements (from different wells) per line were performed. Cell lines with the same genotype were pooled for statistical analysis. Total data points: n = 30 for all samples. Student's t-test ($p < 0.001$). (**E** and **F**) Ribosome structure from PDB ID: 4V6X (Anger et al., 2013). S15 was highlighted, its C-terminal tail is disposed closely to the ribosomal active site. Images were generated by UCSF Chimera (Pettersen et al., 2004). GS: G2019S, WT: wild-type, MC: mutation-corrected, TA: T136A, TD: T136D.